showed electrophysiological and behavioral properties expected of neurons from the midbrain in a rat model of PD (Chung et al., 2006; Kim et al., 2002; Rodriguez-Gomez et al., 2007). Survival of DA neurons obtained in vitro from primate ES cells was also reported in primate hosts (Sanchez-Pernaute et al., 2005; Takagi et al., 2005), but the dopaminergic function of these cells in the primate brain has not been fully evaluated.

Positron emission tomography (PET) is a valuable method for imaging altered DA function in PD. The most common tracer used to visualize and assess the integrity of DA presynaptic systems is 6-[^{18}F]fluoro-L-4-dihydroxyphenylalanine ([^{18}F]FDOPA), a fluoro-analog of 4-dihydroxyphenylalanine (L-dopa). However, uptake of this agent is increased in variable conditions such as inflammation and tumor formation, and assessment of graft function using only this ligand is difficult. The present study therefore used PET with multitracers to analyze both presynaptic and postsynaptic dopaminergic functions and found that transplantation of neural stem cells (NSCs) induced from primate ES cells restored DA function in a primate model of PD.

MATERIALS AND METHODS

Cell culture and differentiation

Astrocyte-conditioned medium (ACM) was prepared by culturing astrocytes obtained from mouse fetal cerebra (Inoue et al., 1988) in DMEM/F12 medium (Invitrogen, Carlsbad, CA) containing N2 supplement (Invitrogen). The CMK6 cynomolgus monkey ES cell line (Suemori et al., 2001) was seeded at a clonal density and grown on a mitomycin C-treated mouse embryonic fibroblast feeder layer in DMEM/F12 medium (Invitrogen) supplemented with 1000 U/ml leukemia inhibitory factor (Chemicon, Temecula, CA), 1 mM β-mercaptoethanol (Invitrogen), and 15% knockout serum replacement (Invitrogen). Colonies of undifferentiated ES cells with a diameter of 300–500 μm and grown for 7–9 days were treated with 0.1% collagenase for 5 min and then detached whole using a glass capillary. Colonies were transferred to nonadhesive bacteriological dishes in ACM supplemented with 20 ng/ml of recombinant human fibroblast growth factor (FGF)-2 (R&D Systems, Minneapolis, MN) and 20 ng/ml of recombinant epidermal growth factor (EGF) (R&D Systems). Colonies were cultured for 10 days, giving rise to floating spheres comprising numerous NSCs. To stimulate proliferation, these spheres were plated onto Matrigel-coated dishes and cultivated for up to 10 days in Neurobasal medium (Invitrogen) supplemented with 2% B-27 (Invitrogen), 20 ng/ml of FGF-2, and 20 ng/ml of EGF. To efficiently induce DA-synthesizing neurons, the medium was replaced with ACM supplemented with 50 ng/ml of sonic hedgehog (Shh; R&D Systems) 1 day before transplantation.

Animals and neurotoxin treatment

All experiments were performed in full compliance with the requirements of the institutional animal care and use committee. Two cynomolgus monkeys (*Macaca fascicularis*), M-1 and M-2, weighing 2.3–2.5 kg were used for the cell therapy experiments. The monkeys were housed under standard conditions of humidity and dark/light cycles with ad libitum access to food and water. To create bilateral striatal lesions, 1-methyl-4-phenyl-1,2,3,6-tetrahydropyridine (MPTP, 0.2–0.4 mg/kg of free base; Sigma-Aldrich Japan K.K., Tokyo, Japan) in phosphate-buffered saline (PBS) was injected intravenously once per week over a 4-month period until a stable parkinsonian syndrome was observed. The total dose of MPTP administered was 1.5 and 2.95 mg/kg. To avoid the possibility of spontaneous recovery from the effects of MPTP, which could mimic the behavioral effect of cell transplantation, the monkeys were allowed to recover for 2 months after the last MPTP treatment.

Transplantation procedures

All surgical procedures were performed in an aseptic environment with the monkeys under isoflurane (1–2%) anesthesia. The head was placed in a stereotaxic device (Kopf Instruments, Tujunga, CA). Each monkey received nine injections of NSCs derived from cynomolgus monkey ES cells (M-1, 1×10^5 viable cells; M-2, 2×10^7 viable cells) in three tracts in the left putamen. NSCs were trypsinized and resuspended in 72 μl of ACM supplemented with Shh. Eight microliters of NSC suspension was injected into each of the nine points using a 50-μl Hamilton microsyringe fitted with a 26-gauge needle over a period of 5 min. The needle was left in place for an additional 3 min to prevent the loss of cells by backflow. As a control, 25 μl of ACM supplemented with Shh was injected into the right putamen. Stereotaxic coordinates of injection sites in the putamen were: Track 1, anterior 13.4 mm, lateral 12 mm, depth +19, 17, 15 mm from the midpoint of the ear bar; Track 2, anterior 16.4 mm, lateral 11.5 mm, depth +20, 18, 16 mm; and Track 3, anterior 18.1 mm, lateral 11 mm, depth +19, 17, 15 mm. From 3 days before surgery, the monkeys received daily intramuscular injections of 0.5 mg/kg of the immunosuppressant FK506 (Astellas Pharmaceuticals, Osaka, Japan) diluted in physiological saline. From 5 days after surgery, the dose was reduced to 0.2 mg/kg for the rest of the experimental period.

PET

Magnetic resonance imaging (MRI) of both monkeys was performed at the National Institute for Physiological Sciences using a 3.0-T imager (Allegra; Sie-

mens, Erlangen, Germany) under pentobarbital anesthesia. Stereotaxic coordinates of PET and MRI were adjusted based on the orbitomeatal (OM) plane with a specially designed head holder. Syntheses of [^{11}C]-labeled-compounds have been described (Tsukada et al., 2000a,b). Data were collected on a high-resolution animal PET scanner (SHR-7700; Hamamatsu Photonics, Hamamatsu, Japan) with a transaxial resolution of 2.6 mm full-width at half-maximum and a center-to-center distance of 3.6 mm (Watanabe et al., 1997). The PET camera allowed 31 slices to be recorded simultaneously. After fasting overnight, the monkey under isoflurane anesthesia was secured to a monkey head folder with stereotaxic coordinates aligned parallel to the OM plane. Each of the [^{11}C]-labeled compounds was delivered through a posterior tibial vein cannula. PET with [^{11}C]L-3,4-dihydroxyphenylalanine (L-[β-^{11}C]DOPA), the precursor of DA synthesis, and [^{11}C]raclopride, a reversible D_2 receptor antagonist, were performed for a total of 64 min with 6 time frames at 10 sec intervals and 12 time frames at 1 min, followed by 16 time frames at 3 min. PET with [^{11}C]2β-carbomethoxy-3β-(4-fluorophenyl)-tropane ([^{11}C]β-CFT) was performed with an additional 19 time frames at 3 min for a total of 91 min. To measure DA release in the striatum indirectly in vivo as reflected by reductions in DA receptor availability, [^{11}C]raclopride was injected through the cannula 30 min after administration of either 0.5 mg/kg of amphetamine or saline. Time-activity curves of each labeled compound in regions of interest chosen from magnetic resonance images were obtained.

For quantification of in vivo binding of [^{11}C]raclopride and [^{11}C]β-CFT, a kinetic 3-compartment analysis method was applied as previously described (Huang et al., 1986). The time-activity curves of plasma and of each region were fitted to a 3-compartment model using the least-squares method. Binding potentials of [^{11}C]raclopride and [^{11}C]β-CFT were calculated by determining the ratio of the estimated k_3 value (association rate) to the estimated k_4 value (dissociation rate). For quantification of L-[β-^{11}C]DOPA utilization rate constant in the striatum of the monkey brain, a graphical analysis method was applied to calculate DA synthesis rate (k_3) as described previously (Tsukada et al., 2000a,b).

Behavioral assessment

Animals were clinically evaluated twice a week using a primate parkinsonism rating scale (PPRS) and activities were recorded on digital videotape. The PPRS is based on the Unified Parkinson's Disease Rating Scale, but was developed specifically for nonhuman primates (Jenner, 2000). On PPRS, scores from 0 (normal) to 4 (maximal disability) are given for each of the six following parkinsonian features: spatial hypokinesia in movements around the cage, bradykinesia, manual dexterity of the right arm, manual dexterity of the left arm, balance, and freezing.

Immunocyto- and immunohistochemistry

Cells cultured on coverslips were fixed with 4% paraformaldehyde in 0.1 M PBS (pH 7.2) for 20 min at 4°C. Cells were then treated with 10% normal horse serum, 2% bovine albumin, and 0.2% Triton X-100 in 0.1 M PBS (pH 7.2) for 20 min at room temperature and incubated further in the presence of the following antibodies separately: nestin (1:200, Chemicon); high-molecular-mass neurofilament protein (NF-H) (1:500, Chemicon); glial fibrillary acidic protein (GFAP) (1:200, Chemicon); O4 (1:200, Chemicon); tyrosine hydroxylase (TH) (1:500, Chemicon); aromatic L-amino acid decarboxylase (AADC) (1:200, Sigma); DA transporter (DAT) (1:200, Chemicon); choline acetyl transferase (ChAT) (1:500 Chemicon); serotonin (5HT) (1:1000, Sigma); and glutamic acid decarboxylase (GAD) (1:1000, Sigma). Cells were washed and then incubated in Alexa Fluor 488- and Alexa Fluor 594-labeled secondary antibodies (1:200; Molecular Probes, Eugene, OR). Cells were mounted in Vectashield containing 4,6-diamidino-2-phenylindole (DAPI; Vector Laboratories, Burlingame, CA) and analyzed under a fluorescence microscope (Eclipse E800; Nikon, Tokyo, Japan) equipped with phase-contrast optics or under a confocal laser-scanning microscope (LSM 510; Carl Zeiss Microimaging Co., Tokyo, Japan). Quantitative immunocytochemical data obtained from 4 to 9 cultures are expressed as mean ± standard error of the mean.

Under deep anesthesia, monkeys were perfused with 4% paraformaldehyde through the ascending aorta. The brains were removed and cut into several blocks 5-mm thick. These blocks were postfixed in the same fixative, left for 3 days in PBS containing 30% sucrose, and then cut on a cryostat into coronal sections 30-μm thick. Sections were treated with 0.3% H_2O_2 for 15 min to inhibit endogenous peroxidase. Sections were incubated at 4°C for 2 days in PBS containing 0.3% Triton X-100 and primary antibodies against mouse monoclonal anti-TH antibody (1:8000; Immnostar, Hudson, WI). Next, sections were incubated in biotinylated antimouse immunoglobulin (Ig)G (1:1000; Vector Laboratories) for 1 h at room temperature, and finally in avidin-biotin-peroxidase complex (1:50; Vector Laboratories) for 30 min at room temperature. Peroxidase activity was revealed in 50 mM Tris-HCl buffer (pH 7.6) containing 0.0004% H_2O_2 and 0.01% 3,3′-diaminobenzidine-4HCl (DAB) (all from Vector Laboratories). For immunofluorescence staining, sections were incubated with mouse monoclonal anti-TH antibody (1:800; Immnostar), rabbit anti-5HT antibody (1:2500; Incstar,

Stillwater, MN), or anti-Ki 67 antibody (1:200; Chemicon) followed by incubation with Alexa Fluor 594-conjugated goat antimouse IgG (1:1000; Molecular Probes). Immunoreactivity was assessed and viewed under confocal laser scanning microscopy (TCS NT; Leica Microsystems, Tokyo, Japan). We estimated TH-immunoreactive (IR) cell counts in serial sections (every 10th) under ×63 magnification on a Zeiss microscope equipped with a video camera.

RESULTS

Efficient induction of DA neurons in culture

A colony of undifferentiated ES cells formed spheres with unique concentric stratiform structure when cultivated in ACM supplemented with FGF-2 and EGF under free-floating conditions, as reported previously (Nakayama et al., 2003, 2004). These spheres displayed peripheral NSCs with a center of proliferating ES cells. Subsequent culture on an adhesive substrate formed circular clusters of cells from which many nestin-positive NSCs migrated. After a few passages, almost all cells expressed nestin (99.5% ± 0.5%) and only a few cells (<0.5%) expressed NF-H. To examine differentiation properties in vitro, a small fraction of NSCs were grown in ACM with Shh. After 5 days, cells in culture displayed a neuronal appearance with long neuritis and became positive for NF-H (99.5% ± 0.5%). Cells were immunoreactive for neither antibody against the astrocyte marker GFAP nor the antibody against oligodendrocyte protein O4 (data not shown). Moreover, many (70% ± 1%) NF-H-positive cells expressed DA neuronal markers such as TH, AADC, and DAT (Fig. 1). Small proportions of NF-H-positive cells expressed either 5HT (12.2% ± 1.3%), ChAT (1.0% ± 0.6%), or GAD (11.9% ± 1.6%).

DA production is restored in the grafted putamen

We used PET to assess nigrostriatal dopaminergic function in MPTP-treated monkeys before and after NSC implantation. MPTP-intoxicated monkeys displayed comprehensive loss of uptake for L-[β-^{11}C]DOPA, a substrate for AADC, and [^{11}C]β-CFT, a DA transporter ligand, in both hemispheres of the brain before transplantation, suggesting severe loss of DA terminals (Figs. 2A and 2B). At 4 weeks postoperatively, we found increases in both L-[β-^{11}C]DOPA and [^{11}C]β-CFT uptake in the grafted putamen. Quantitative analysis of scans at 4 weeks after implantation revealed significant increases in both L-[β-^{11}C]DOPA uptake (M-1, 41%; M-2, 61%) and [^{11}C]β-CFT uptake (M-1, 33%; M-2, 36%) in the implanted striatum compared with the control putamen (Figs. 2C and 2D). The degree of decrease in striatal radioactivity from [^{11}C]raclopride after amphetamine challenge in M-2 was significantly higher in the grafted putamen (16%) than in the control putamen (0.6%), indicating increased release of DA in the striatum (Fig. 3).

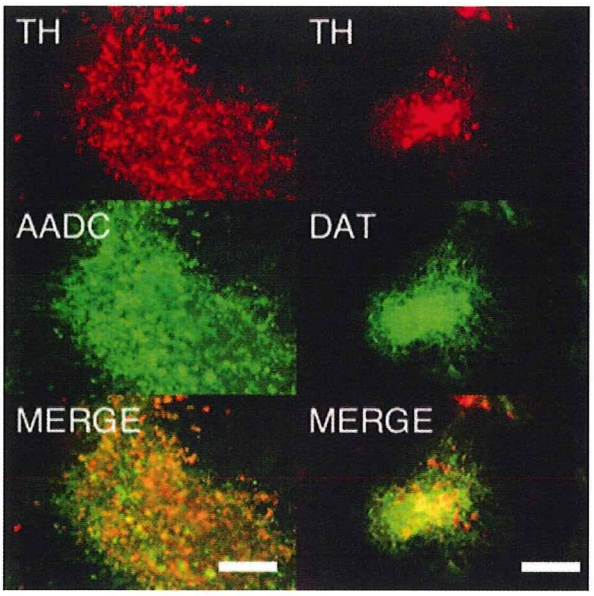

Fig. 1. Neurons derived from ES cells show markers of DA-synthesizing cells. Dual labeling with antityrosine hydroxylase (TH) and antiaromatic L-amino acid decarboxylase (AADC) antibodies shows coexpression of dopamine (DA)-synthesizing enzymes in the neurons. Dual labeling with anti-TH and anti-DA transporter (DAT) antibodies indicates the DA phenotype. Scale bar: 50 μm.

Behavioral recovery is modest

After chronic administration of MPTP, monkeys developed bilateral parkinsonism manifested by a loss of spontaneous motor activity, bradykinesia, impairment of manual dexterity, tremor, and freezing. Parkinsonian features were stable for 2 months from the last MPTP treatment. Three months after unilateral cell transplantation into the putamen, both monkeys showed modest behavioral improvements demonstrated by both PPRS and systematic analysis of digital videotapes. Before MPTP treatment, both monkeys scored 0 on PPRS. After MPTP, but before implantation, mean scores of four evaluations on the PPRS were 14 for M-1 and 12 for M-2. At 12 weeks after implantation, this score reduced to 11 and 10, respectively. In M-2, the score remained constant during the observation period until 6 months after implantation. Regardless of on- or off-medication, no dyskinesia was observed.

Grafted cells differentiate into TH-positive cells in the brain

Histological assessment of brains was performed for M-1 and M-2 at 3 and 6 months after implantation,

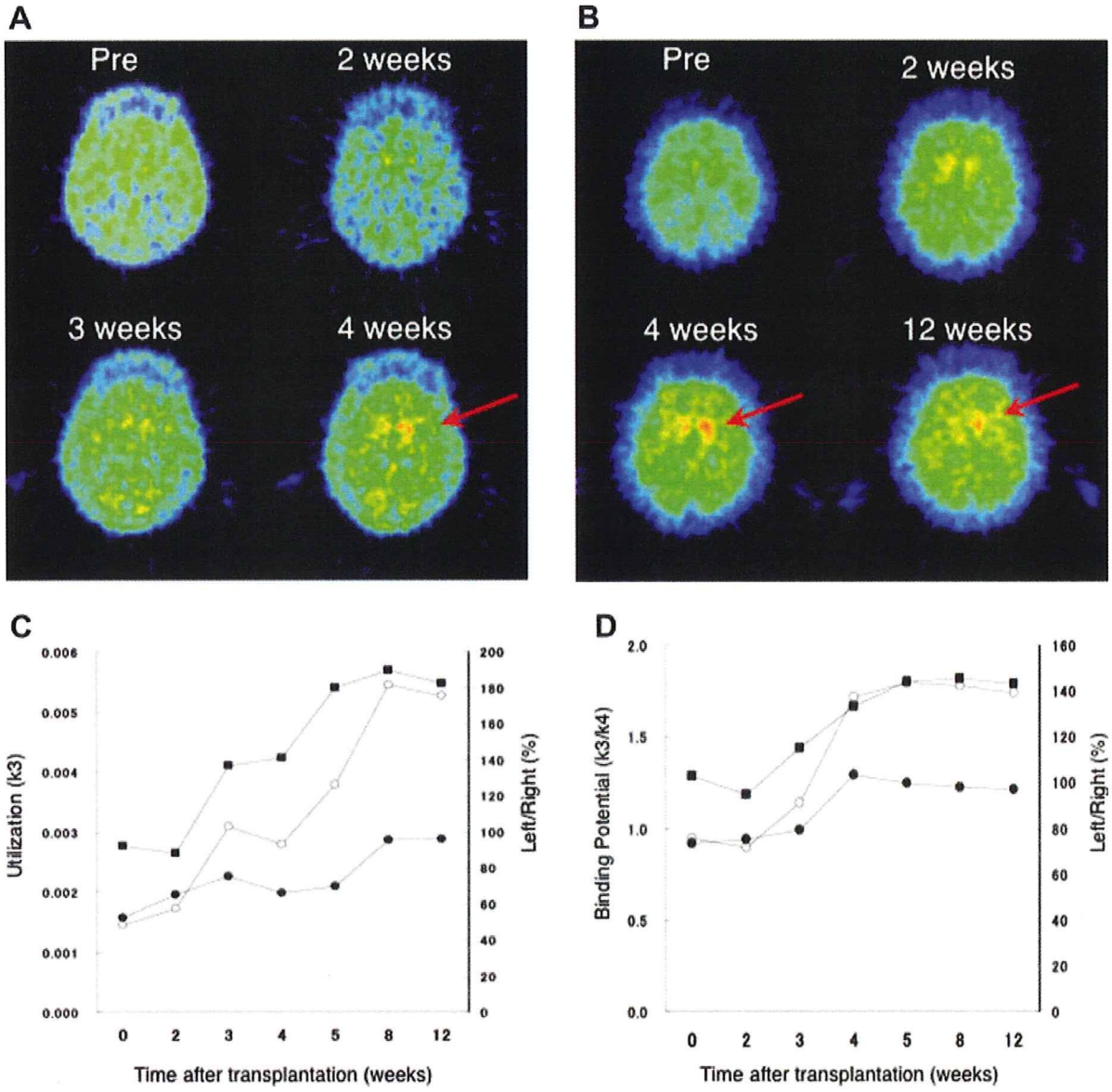

Fig. 2. (**A**, **B**) PET images of L-[β-^{11}C]DOPA (A) and [^{11}C]β-CFT (B) uptake in monkey M-1 before and after cell transplantation. Four weeks after implantation, increased radionuclide uptake was detected in the implanted putamen (arrows). (**C**, **D**) Graphic representation of relative changes in signal strength over time in the same animal, showing significant increases in L-[β-^{11}C]DOPA utilization (k_3 value) (C) and [^{11}C]β-CFT binding potential (BP) (k_3/k_4 value) (D) in the implanted (left: open circles) putamen compared with control (right: filled circles) putamen. Filled squares indicate left to right ratio.

respectively. Many TH-IR cells, about 1000 in M-1 and 3000 in M-2, thrived in the grafted putamen (Fig. 4). Less than 50 TH-IR cells were found in the putamen on the side contralateral to the graft. A small number of 5HT-IR cells was identified in the grafted putamen (<5 cells). No TH-positive cells were positive for the proliferation marker Ki-67. Hematoxylin and eosin staining showed no signs of teratoma-like structures in the transplanted putamen.

DISCUSSION

This study demonstrated with PET that engraftment of NSCs derived from primate ES cells has the capacity to restore DA function in a primate model of PD. Transplantation of neural precursors has become one of the key strategies for cell replacement in the brain. To bypass the shortage of donor tissue, a wide range of experimental approaches have been studied, including proliferation of NSCs in vitro stimulated by

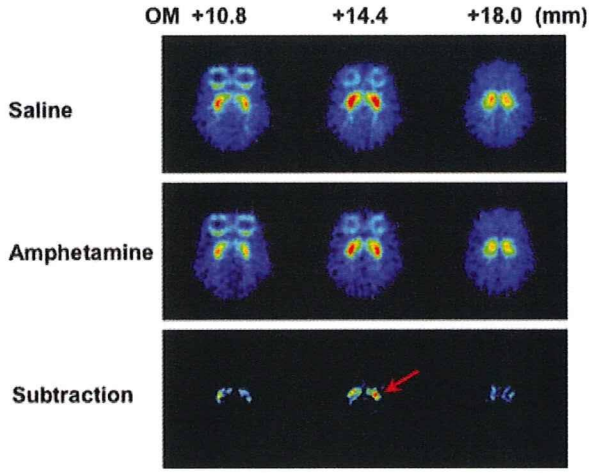

Fig. 3. Drug-induced release of DA in the grafted striatum 12 weeks after transplantation in monkey M-2. After methamphetamine administration, [^{11}C]raclopride binding in the implanted putamen was significantly reduced compared with that in the control putamen. Each slice image after methamphetamine infusion (middle row) was subtracted from a corresponding baseline image (upper row). Subtraction images (lower row). The images of each column are in horizontal plane and same stereotaxic coordinates (mm) from the orbitomeatal (OM) line. Arrows indicate the side of the implant.

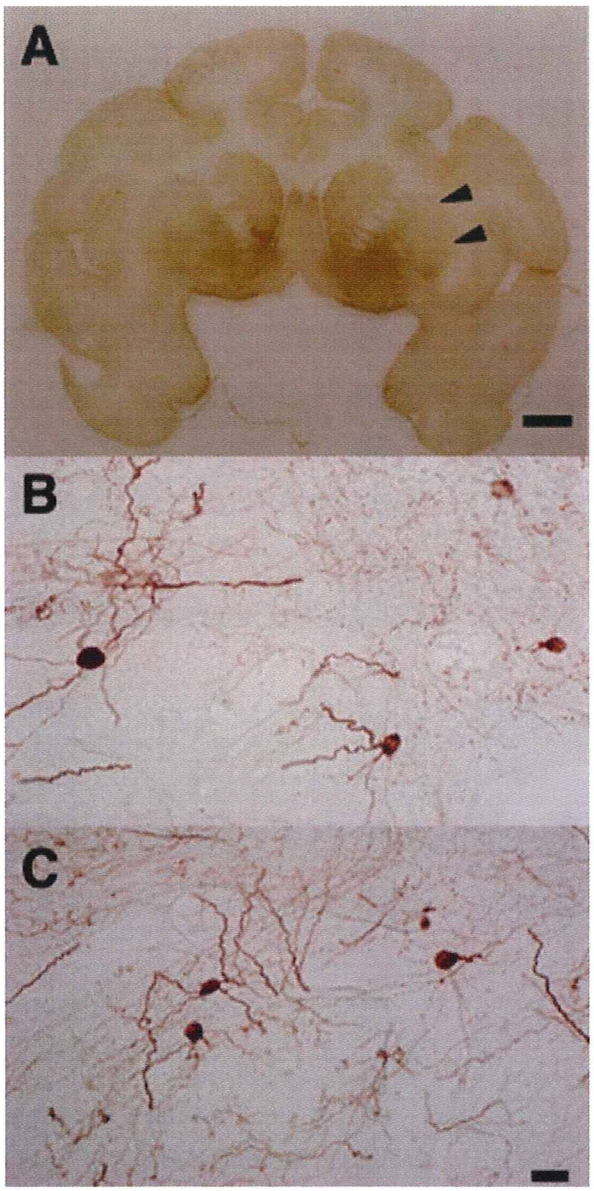

Fig. 4. TH-IR cells in the unilateral putamen of monkey M-1 at 3 months after cell implantation. (**A**) Restoration of TH-IR in the implanted putamen (arrowhead) is not obvious at low magnification. However, TH-IR neurons are apparent in dorsal (**B**) and ventral (**C**) portions of the implanted putamen. Scale bar: 0.5 cm (A); 20 μm (B, C).

mitogen treatment, ex vivo introduction of growth stimulating oncogenes, xenotransplantation, enhancement of endogenous adult neurogenesis, and attempts to recruit non-neural adult stem cells from other tissues (Hall et al., 2007; Liu, 2008). However, in addition to the limited plasticity and slow propagation of adult stem cells, continuous expression of oncogenes or stimulation of mitogens raises question about the long-term safety of these strategies. Of the various candidate donor cells, ES cells are the most attractive due to the characteristics of pluripotency and the potential for unlimited self-renewal. Although human ES cells seem promising for clinical applications, an alternative model system based on ES cells derived from nonhuman primates is necessary for preclinical studies, including allogenic transplantation.

The present study used cynomolgus monkey ES cells that resemble human ES cells but are distinct from murine ES cells in terms of morphology, expression of surface markers and feeder- and leukemia inhibitory factor-dependence, among other factors (Suemori et al., 2001). We have previously shown that astrocyte-derived factors instruct mouse and primate ES cells to differentiate into neurons quickly and efficiently (Nakayama et al., 2003, 2004). This ACM method is superior to previous methods in terms of simplicity, efficiency, and productivity of neural differentiation. The number of cells was increased 1000-fold, along with differentiation from ES cells into NSCs. NSCs can be highly purified without using either magnetic- or fluorescence-activated cell sorting, and incorporation of undifferentiated ES cells is virtually eliminated. Although low doses of undifferentiated mouse ES cells transplanted into rat striatum developed into fully differentiated DA neurons (Bjorklund et al., 2002), elimination of undifferentiated ES cells is crucial for reducing the risk of tumor formation. Consistent with our previous observations,

culture of NSCs derived from cynomolgus monkey ES cells on an adhesive substrate in ACM exclusively promoted differentiation into neurons.

Parkinsonian features were induced by intravenous administration of MPTP over a period of several months. MPTP causes slowly progressive loss of DA neurons in the substantia nigra, resulting in primates showing all the clinical signs of PD, including tremor, rigidity, akinesia, and postural instability (Wichmann and DeLong, 2003). We created bilateral striatal lesions but implanted cells unilaterally, so one side could serve as a control. Functional effects of the graft were evaluated by comparing PET images of the implanted putamen with those of the contralateral putamen. PET can be used to assess DA function in vivo (Brooks, 2004) by following increases in L-[β-^{11}C]DOPA uptake or [^{11}C]β-CFT binding, which are attributable to the expression of AADC and storage of DA in the putamen and thus indicate graft survival and development of DA neurons. In addition, functional DA release from the graft was demonstrated by imaging D_2 receptor occupancy. Degrees of decrease in striatal radioactivity of [^{11}C]raclopride after amphetamine challenge were significantly higher in the grafted putamen. Based on microdialysis studies, a 1% change in striatal [^{11}C]raclopride binding has been estimated to correspond to a $\geq$8% change in synaptic DA levels (Breier et al., 1997). We identified numerous TH neurons in the grafted putamen. Although small populations of TH neurons may be found in the primate striatum after creating lesions of the nigrostriatal dopaminergic pathways, most are located in the caudate and precommissural putamen (Mazloom and Smith, 2006). The dramatic increase in the number of TH-IR cells in the postcommissural putamen suggests that these TH-IR cells were derived from the graft and contributed to the restoration of dopaminergic function.

Behavioral recovery was modest at 12 weeks after implantation. More DA neurons and synaptic DA release might be necessary for apparent behavioral recovery. Improving neuronal survival and increasing axonal outgrowth would possibly improve the magnitude of the response to grafting. In this regard, the combination of cell replacement and neuroprotective strategies by gene delivery may be effective in preventing the loss of endogenous and grafted NSCs. Another possible explanation for incomplete behavioral recovery is that functional integration of DA neurons with the host circuitry may take place gradually. PD patients with implanted fetal DA neurons show continuous symptomatic improvements even after DA storage capacity in the striatum (measured by L-[β-^{11}C]DOPA PET) and response to DA-releasing agents has plateaued (Isacson et al., 2001; Piccini et al., 2000). With bilateral implantation, further amelioration of global parkinsonism (including enhanced spontaneous activity and improved balance) would be expected, since only 20% of thalamic projections from the basal ganglia are crossed in monkeys (Parent and Hazrati, 1995) and unilateral implantation would mainly affect contralateral limb movement. Monkeys did not display dyskinesia with or without L-dopa. This result supports previous observations that functional DA grafts do not independently generate abnormal DA responses (Bjorklund et al., 2002).

Given the recent successful isolation of nuclear-transferred ES cell lines (Tabar et al., 2008), our findings of efficient ES cell transplantation, expansion, and differentiation into functional DA neurons in the primate model have implications for ES cells as a donor source for cell therapy against PD.

ACKNOWLEDGMENTS

The authors thank Astellas Pharmaceuticals (Osaka, Japan) for providing FK506.

REFERENCES

Bjorklund LM, Sanchez-Pernaute R, Chung S, Andersson T, Chen IY, McNaught KS, Brownell AL, Jenkins BG, Wahlestedt C, Kim KS, Isacson O. 2002. Embryonic stem cells develop into functional dopaminergic neurons after transplantation in a Parkinson rat model. Proc Natl Acad Sci USA 99:2344–2349.

Breier A, Su TP, Saunders R, Carson RE, Kolachana BS, de Bartolomeis A, Weinberger DR, Weisenfeld N, Malhotra AK, Eckelman WC, Pickar D. 1997. Schizophrenia is associated with elevated amphetamine-induced synaptic dopamine concentrations: Evidence from a novel positron emission tomography method. Proc Natl Acad Sci USA 94:2569–2574.

Brooks DJ. 2004. Positron emission tomography imaging of transplant function. NeuroRx 1:482–491.

Chung S, Shin BS, Hwang M, Lardaro T, Kang UJ, Isacson O, Kim KS. 2006. Neural precursors derived from embryonic stem cells, but not those from fetal ventral mesencephalon, maintain the potential to differentiate into dopaminergic neurons after expansion in vitro. Stem Cells 24:1583–1593.

Hall VJ, Li JY, Brundin P. 2007. Restorative cell therapy for Parkinson's disease: A quest for the perfect cell. Semin Cell Dev Biol 18:859–869.

Huang SC, Barrio JR, Phelps ME. 1986. Neuroreceptor assay with positron emission tomography: Equilibrium versus dynamic approaches. J Cereb Blood Flow Metab 6:515–521.

Inoue N, Matsui H, Tsukui H, Hatanaka H. 1988. The appearance of a highly digitalis-sensitive isoform of Na+,K+-ATPase during maturation in vitro of primary cultured rat cerebral neurons. J Biochem (Tokyo) 104:349–354.

Isacson O, Bjorklund L, Pernaute RS. 2001. Parkinson's disease: Interpretations of transplantation study are erroneous. Nat Neurosci 4:553.

Jenner P. 2000. Factors influencing the onset and persistence of dyskinesia in MPTP-treated primates. Ann Neurol 47 (4 Suppl 1): S90–S99; discussion S99–S104.

Kim JH, Auerbach JM, Rodriguez-Gomez JA, Velasco I, Gavin D, Lumelsky N, Lee SH, Nguyen J, Sanchez-Pernaute R, Bankiewicz K, McKay R. 2002. Dopamine neurons derived from embryonic stem cells function in an animal model of Parkinson's disease. Nature 418:50–56.

Kish SJ, Shannak K, Hornykiewicz O. 1988. Uneven pattern of dopamine loss in the striatum of patients with idiopathic Parkinson's disease. Pathophysiologic and clinical implications. N Engl J Med 318:876–880.

Li JY, Christophersen NS, Hall V, Soulet D, Brundin P. 2008. Critical issues of clinical human embryonic stem cell therapy for brain repair. Trends Neurosci 31:146–153.

Liu SV. 2008. iPS cells: A more critical review. Stem Cells Dev 17:391–397.

Mazloom M, Smith Y. 2006. Synaptic microcircuitry of tyrosine hydroxylase-containing neurons and terminals in the striatum

of 1-methyl-4-phenyl-1,2,3,6-tetrahydropyridine-treated monkeys. J Comp Neurol 495:453–469.
Nakayama T, Momoki-Soga T, Inoue N. 2003. Astrocyte-derived factors instruct differentiation of embryonic stem cells into neurons. Neurosci Res 46:241–249.
Nakayama T, Momoki-Soga T, Yamaguchi K, Inoue N. 2004. Efficient production of neural stem cells and neurons from embryonic stem cells. Neuroreport 15:487–491.
Newman MB, Bakay RA. 2008. Therapeutic potentials of human embryonic stem cells in Parkinson's disease. Neurotherapeutics 5:237–251.
Parent A, Hazrati LN. 1995. Functional anatomy of the basal ganglia. I. The cortico-basal ganglia-thalamo-cortical loop. Brain Res Brain Res Rev 20:91–127.
Piccini P, Lindvall O, Bjorklund A, Brundin P, Hagell P, Ceravolo R, Oertel W, Quinn N, Samuel M, Rehncrona S, Widner H, Brooks DJ. 2000. Delayed recovery of movement-related cortical function in Parkinson's disease after striatal dopaminergic grafts. Ann Neurol 48:689–695.
Rodriguez-Gomez JA, Lu JQ, Velasco I, Rivera S, Zoghbi SS, Liow JS, Musachio JL, Chin FT, Toyama H, Seidel J, Green MV, Thanos PK, Ichise M, Pike VW, Innis RB, McKay RD. 2007. Persistent dopamine functions of neurons derived from embryonic stem cells in a rodent model of Parkinson disease. Stem Cells 25:918–928.
Sanchez-Pernaute R, Studer L, Ferrari D, Perrier A, Lee H, Vinuela A, Isacson O. 2005. Long-term survival of dopamine neurons derived from parthenogenetic primate embryonic stem cells (cyno-1) after transplantation. Stem Cells 23:914–922.
Suemori H, Tada T, Torii R, Hosoi Y, Kobayashi K, Imahie H, Kondo Y, Iritani A, Nakatsuji N. 2001. Establishment of embryonic stem cell lines from cynomolgus monkey blastocysts produced by IVF or ICSI. Dev Dyn 222:273–279.
Tabar V, Tomishima M, Panagiotakos G, Wakayama S, Menon J, Chan B, Mizutani E, Al-Shamy G, Ohta H, Wakayama T, Studer L. 2008. Therapeutic cloning in individual parkinsonian mice. Nat Med 14:379–381.
Takagi Y, Takahashi J, Saiki H, Morizane A, Hayashi T, Kishi Y, Fukuda H, Okamoto Y, Koyanagi M, Ideguchi M, Hayashi H, Imazato T, Kawasaki H, Suemori H, Omachi S, Iida H, Itoh N, Nakatsuji N, Sasai Y, Hashimoto N. 2005. Dopaminergic neurons generated from monkey embryonic stem cells function in a Parkinson primate model. J Clin Invest 115:102–109.
Tsukada H, Harada N, Nishiyama S, Ohba H, Kakiuchi T. 2000a. Cholinergic neuronal modulation alters dopamine D2 receptor availability in vivo by regulating receptor affinity induced by facilitated synaptic dopamine turnover: Positron emission tomography studies with microdialysis in the conscious monkey brain. J Neurosci 20:7067–7073.
Tsukada H, Harada N, Nishiyama S, Ohba H, Sato K, Fukumoto D, Kakiuchi T. 2000b. Ketamine decreased striatal [(11)C]raclopride binding with no alterations in static dopamine concentrations in the striatal extracellular fluid in the monkey brain: Multiparametric PET studies combined with microdialysis analysis. Synapse 37:95–103.
Watanabe M, Okada H, Shimizu K, Omura T, Yoshikawa E, Kosugi T, Mori S, Yamashita T. 1997. A high resolution animal PET scanner using compact PS-PMT detectors. IEEE Trans Nucl Sci 44:1277–1282.
Wichmann T, DeLong MR. 2003. Pathophysiology of Parkinson's disease: The MPTP primate model of the human disorder. Ann N Y Acad Sci 991:199–213.

Cell Transplantation, Vol. 18, pp. 381–389, 2009
Printed in the USA.

0963-6897/09 $90.00 + .00
E-ISSN 1555-3892
www.cognizantcommunication.com

ERas Is Expressed in Primate Embryonic Stem Cells But Not Related to Tumorigenesis

Yujiro Tanaka,*¶[1] Tamako Ikeda,*[1] Yukiko Kishi,* Shigeo Masuda,* Hiroaki Shibata,*‡ Kengo Takeuchi,§ Makoto Komura,¶ Tadashi Iwanaka,¶ Shin-ichi Muramatsu,† Yasushi Kondo,# Kazutoshi Takahashi,** Shinya Yamanaka,** and Yutaka Hanazono*

*Division of Regenerative Medicine, Center for Molecular Medicine, Jichi Medical University, Tochigi, Japan
†Division of Neurology, Department of Internal Medicine, Jichi Medical University, Tochigi, Japan
‡Tsukuba Primate Research Center, National Institute of Biomedical Innovation, Ibaraki, Japan
§Department of Pathology, Cancer Institute Hospital, Tokyo, Japan
¶Department of Pediatric Surgery, Graduate School of Medicine, University of Tokyo, Tokyo, Japan
#Mitsubishi Tanabe Pharma, Osaka, Japan
**Center for iPS Cell Research and Application, Institute for Integrated Cell-Material Sciences, Kyoto University, Kyoto, Japan

The ERas gene promotes the proliferation of and formation of teratomas by mouse embryonic stem (ES) cells. However, its human orthologue is not expressed in human ES cells. This implies that the behavior of transplanted mouse ES cells would not accurately reflect the behavior of transplanted human ES cells and that the use of nonhuman primate models might be more appropriate to demonstrate the safety of human ES cell-based therapies. However, the expression of the ERas gene has not been examined in nonhuman primate ES cells. In this study, we cloned the cynomolgus homologue and showed that the ERas gene is expressed in cynomolgus ES cells. Notably, it is also expressed in cynomolgus ES cell-derived differentiated progeny as well as cynomolgus adult tissues. The ERas protein is detectable in various cynomolgus tissues as assessed by immunohistochemisty. Cynomolgus ES cell-derived teratoma cells, which also expressed the ERas gene at higher levels than the undifferentiated cynomolgus ES cells, did not develop tumors in NOD/Shi-*scid*, IL-2Rγ^{null} (NOG) mice. Even when the ERas gene was overexpressed in cynomolgus stromal cells, only the plating efficiency was improved and the proliferation was not promoted. Thus, it is unlikely that ERas contributes to the tumorigenicity of cynomolgus cells. Therefore, cynomolgus ES cells are more similar to human than mouse ES cells despite that ERas is expressed in cynomolgus and mouse ES cells but not in human ES cells.

Key words: Embryonic stem cell; ERas; Cynomolgus monkey; Tumorigenesis

INTRODUCTION

The ERas gene promotes the growth of and formation of teratomas by mouse ES cells by producing a constitutively active ERas protein and is not expressed in mouse ES cell-derived differentiated progeny or mouse tissues (22). Disruption of the ERas gene in mouse ES cells by homologous recombination results in a significantly reduced proliferation rate and a reduced tumorigenic potential without loss of pluripotency (22). Although the ERas gene is expressed in divergent species such as mice, dogs, and cows, it is not expressed in humans (1,12,17). Its inactivation is likely a relatively recent event in mammalian evolution. It is intriguing to speculate that some of the differences in the proliferation rate or other properties of mouse and human ES cells (9,13) are related to the differences in expression of this constitutively active ERas gene. It may also imply that the behavior of transplanted mouse ES cells does not accurately reflect the behavior of transplanted human ES cells and that the use of nonhuman primate models (11,21,25) would be more appropriate to demonstrate the safety (tumorigenicity) of human ES cell-based therapies (12). However, the expression of the ERas gene has not been examined in nonhuman primate ES cells (19,24). Here, we show that the ERas gene is expressed

Received July 18, 2008; final acceptance October 21, 2008. Online prepub date: April 15, 2009.
[1]Equal contribution.
Address correspondence to Yutaka Hanazono, M.D., Ph.D., Professor, Division of Regenerative Medicine, Center for Molecular Medicine, Jichi Medical University, 3311-1 Yakushiji, Shimotsuke, Tochigi 329-0498, Japan. Tel: +81-285-58-7451; Fax: +81-285-44-5205; E-mail: hanazono@jichi.ac.jp

in cynomolgus ES cells unlike human ES cells. In addition, the ERas gene is widely expressed in adult cynomolgus tissues. However, its forced expression in cynomolgus cells even at high levels was not related to tumorigenesis. Therefore, cynomolgus ES cells are more similar to human than mouse ES cells despite that ERas is expressed in cynomolgus and mouse ES cells but not in human ES cells.

MATERIALS AND METHODS

Cell Culture and Differentiation

A cynomolgus ES cell line (CMK6) (19), its subline (CMK6G) stably expressing enhanced green fluorescent protein (EGFP) (20), and a human ES cell line (SA181, Cellartis AB, Göteborg, Sweden) (10) were maintained on a feeder layer of mitomycin C (Kyowa, Tokyo, Japan)-treated mouse (BALB/c, Clea, Tokyo, Japan) embryonic fibroblasts (MEFs) as previously described (10,19). Confluent ES cells were dissociated from the feeder layer using 0.1% collagenase type IV (Invitrogen, Carlsbad, CA, USA). Cynomolgus stromal cells were obtained from cultured adherent cells of cynomolgus bone marrow.

For neural differentiation from cynomolgus ES cells, astrocyte-conditioned medium (ACM) was prepared by culturing astrocytes obtained from mouse fetal cerebra in Dulbecco's modified Eagle's medium (DMEM)/F12 medium containing an N2 supplement (Invitrogen) (15). Colonies of cynomolgus ES cells (800–1000 μm in diameter) were plucked from the feeder layer using a glass capillary and transferred into nonadhesive bacteriological dishes each containing ACM supplemented with 20 ng/ml of recombinant human fibroblast growth factor-2 (FGF-2) (R&D, Minneapolis, MN, USA). The colonies were cultured for 12 days, giving rise to neural stem cells, which were plated onto poly-L-lysine/laminin (Sigma-Aldrich, St. Louis, MO, USA)-coated dishes and cultivated for 7 days in Neurobasal medium supplemented with 2% B-27 (both from Invitrogen), 20 ng/ml of FGF-2, and 20 ng/ml of recombinant human epidermal growth factor (R&D). After the medium was replaced with ACM and 14 days of culture, the neural stem cells differentiated into neurons (16).

ERas Cloning and Transfection

Based on the human ERas cDNA sequence in Genbank (accession No. NM 181532), the primer set 5′-CAT GGA GCT GCC AAC AAA GCC TG-3′ and 5′-TGT GTC CCT CAA AGC TAG TTG CCT-3′ was designed for the cynomolgus ERas' complete coding sequence. Total RNA was extracted from cynomolgus ES cells using the EZ1 RNA universal tissue kit (Qiagen, Hilden, Germany) with RNase-Free DNase Set (Qiagen), and reverse-transcribed using the RNA LA PCR kit (Takara, Shiga, Japan) with an oligo dT primer. The resulting cDNA was subjected to PCR with this primer set. The PCR product was sequenced with the ABI Prism 310 (Applied Biosystems, Foster, CA, USA). The sequence analysis was performed with Genetyx-Mac software (Genetyx Corporation, Tokyo, Japan). We previously constructed the plasmids pPyCAG-EGFP-gw-IP (expressing EGFP) and pPyCAG-EGFP-gw-IP-mouse ERas (expressing EGFP-mERas) (22). The cDNA encoding the human or cynomolgus ERas gene was inserted into pPyCAG-EGFP-gw-IP to construct pPyCAG-EGFP-gw-IP-human ERas (expressing EGFP-human ERas) or pPyCAG-EGFP-gw-IP-cynomolgus ERas (expressing EGFP-cynomolgus ERas), respectively. The insert was confirmed by DNA sequencing. The plasmids were transfected into cynomolgus stromal cells using Lipofectamin 2000 (Invitrogen). The transfected cells were selected in the presence of puromycin (5 μg/ml).

Transplantation

Cells (1×10^7/site) were transplanted into the thigh muscle of immunodeficient NOD/Shi-*scid*, IL-2Rγ^{null} (NOG) mice which were purchased from Central Institute for Experimental Animals (Kanagawa, Japan). Cynomolgus ES cell-derived teratomas were generated after in utero transplantation of cynomolgus ES cells into fetal sheep as described previously (23). Adherent cells from the teratomas were propagated in DMEM (Sigma-Aldrich) supplemented with 10% fetal bovine serum (FBS) (HyClone, Logan, UT, USA). All experiments were performed in accordance with the Jichi Medical University Guide for Laboratory Animals. Experimental procedures were approved by the Animal Care and Use Committee of Jichi Medical University.

Reverse Transcription (RT)-PCR

cDNA was prepared from each sample as mentioned above and subjected to PCR with the following primer sets: for Oct-4, 5′-GGA CAC CTG GCT TCG GAT T-3′ and 5′-TTC GCT TTC TCT TTC GGG C-3′; and for glyceraldehyde-3-phosphate dehydrogenase (GAPDH), 5′-CCC TGG CCA AGG TCA TCC ATG ACA AC-3′ and 5′-CCA GTG AGC TTC CCG TTC AG-3′. Amplification conditions were 30 cycles of 95°C for 60 s, 58°C for 60 s, and 72°C for 60 s. PCR without the initial RT was also conducted to rule out DNA contamination. For real-time quantitative RT-PCR, a QuantiTect SYBR Green PCR kit (Qiagen) and the ABI Prism 7000 (Applied Biosystems) were used, and amplification conditions were 40 cycles of 95°C for 60 s, 58°C for 60 s, and 72°C for 60 s. The gene expression levels were adjusted based on those of the internal control GAPDH.

Immunoblotting

Preparation of cell lysates and Western blot analyses were performed as described previously (22). Briefly, cells (1×10^7) were washed twice with ice-cold phosphate-buffered saline (PBS) and suspended in the buffer containing 10 mM Tris-HCl (pH 7.5), 1 mM $MgCl_2$, and the 1× Complete Protease Inhibitors (Roche, Basel, Switzerland), followed by incubation on ice for 30 min. These samples were disrupted with Dounce tissue homogenizer (Wheaton, NJ, USA) and added with 1 M NaCl to a final concentration of 150 mM. For lysis, these samples were added with a final concentration of 5% SDS, 1% NP-40, and 1% deoxicorate acids, followed by incubation on ice for 10 min. The samples were then centrifuged at $12,000 \times g$ for 30 min at 4°C, and supernatants were collected. The protein concentrations were measured by the Bio-Rad Bradford assay (BioRad Laboratories, CA, USA). An equal amount of protein (10 μg per lane) was electrophoresed on 12.5% polyacrylamide gel (Atto, Tokyo, Japan) and blotted onto a PVDF membrane (Immobiron; Millipore, MA, USA). The membrane was blocked by TBST containing 5% w/v Amersham ECL-Blocking Agent (GE Healthcare, Buckinghamshire, UK) and then incubated with rabbit antiserum against mouse ERas (22) overnight at 4°C. After washed with TBST, the membrane was incubated with anti-rabbit IgG HRP (Jackson Laboratory, CA, USA) at room temperature for 60 min. Signal was detected using Amersham ECL Plus Western Blotting Detection reagents (GE Healthcare) according to the manufacturer's protocol and visualized on the LAS 3000 mini (Fujifilm, Tokyo, Japan).

Immunohistochemistry

For the immunofluorescent staining of frozen sections, tissues were fixed with 4% paraformaldehyde. The sections were labeled with rabbit anti-serum against mouse ERas (22). The primary antibody (Ab) was detected with a Tyramide Signal Amplification Kit (Invitrogen). After nuclei were stained with DAPI (Donjindo, Kumamoto, Japan), the sections were observed with a confocal laser scanning microscope (Olympus, Tokyo, Japan). For immunohistochemistry, tissues were fixed with 4% paraformaldehyde and embedded in paraffin. To identify GFP-positive cells, the sections were stained with rabbit anti-GFP Ab (Clontech, Palo Alto, CA, USA), reacted with the Dako EnVision+ System HRP (Dako, Copenhagen, Denmark), and visualized with 3,3′-diaminobenzide tetrahydrochloride (Dojindo). Nuclei were counterstained with hematoxylin.

Flow Cytometry

The expression of GFP and ERas was analyzed using a FACS Calibur flow cytometer (BD Pharmingen, San Diego, CA, USA). To detect ERas, cells were fixed using fixation/permeabilization buffer (eBioscience, San Diego, CA, USA) for 2 h at 4°C and then incubated with Alexa Fluor 647 (Invitrogen)-conjugated rabbit antiserum against ERas for 60 min at 4°C. Data acquisition and analysis were performed using CellQuest software (BD Pharmingen). Fluorescence-conjugated, irrelevant Abs served as negative controls.

Cell Proliferation Assay

Total cell numbers and proliferating cell numbers were measured with Cell Counting Kit-8 (Dojindo) and with Cell Proliferation ELISA, BrdU (colorimetric) (Roche), respectively. For Cell Counting Kit-8, cells were seeded in 96-well plates at 5×10^3 per well and measured after 6, 24, 36, 48, and 80 h of incubation according to the manufacturer's instructions. For Cell Proliferation ELISA, cells were seeded in 96-well plates at 2×10^3 per well and measured after 24, 36, 48, 72, and 96 h of incubation. Significant differences were examined using the *t*-test.

RESULTS AND DISCUSSION

Cynomolgus Cells and Tissues Express ERas

We first cloned and sequenced the cynomolgus orthologue of the ERas gene from cDNA of the undifferentiated cynomolgus ES cells (Fig. 1A). The translated amino acid sequence showed a higher degree of homology to human than mouse ERas (99% vs. 75%) (Fig. 1B). We could not detect the ERas protein in cynomolgus ES cells by flow cytometry, implying its weak expression (data not shown).

Next, we examined the expression of the ERas gene in adult cynomolgus tissues by RT-PCR. Using a primer set to cover the entire coding region, the amplicons from all nine somatic tissues were the same size as that from cynomolgus ES cells (Fig. 2A). The PCR product was sequenced to confirm that it was the ERas gene. This clearly shows that a full-length version of the ERas gene is transcribed in cynomolgus tissues, despite that ERas is not expressed in mouse tissues (22).

We then examined the protein expression in adult cynomolgus tissues by immunohistochemistry. Immunoblotting revealed that the antibody reacts to human and cynomolgus ERas as well as mouse ERas, although the antibody was generated against recombinant mouse ERas (22) (Fig. 2B). In addition, it specifically reacts to ERas (25 kDa) and does not react to other Ras family proteins (N-, H-, or K-Ras; 21 kDa) in cynomolgus cells expressing these Ras genes (Fig. 2B). Using this antibody, we detected ERas-positive cells in all tissues tested (brain, thymus, intestine, and ovary) (Fig. 2C). At a higher magnification, it turned out that ERas is localized on the cytoplasmic membrane as expected (Fig.

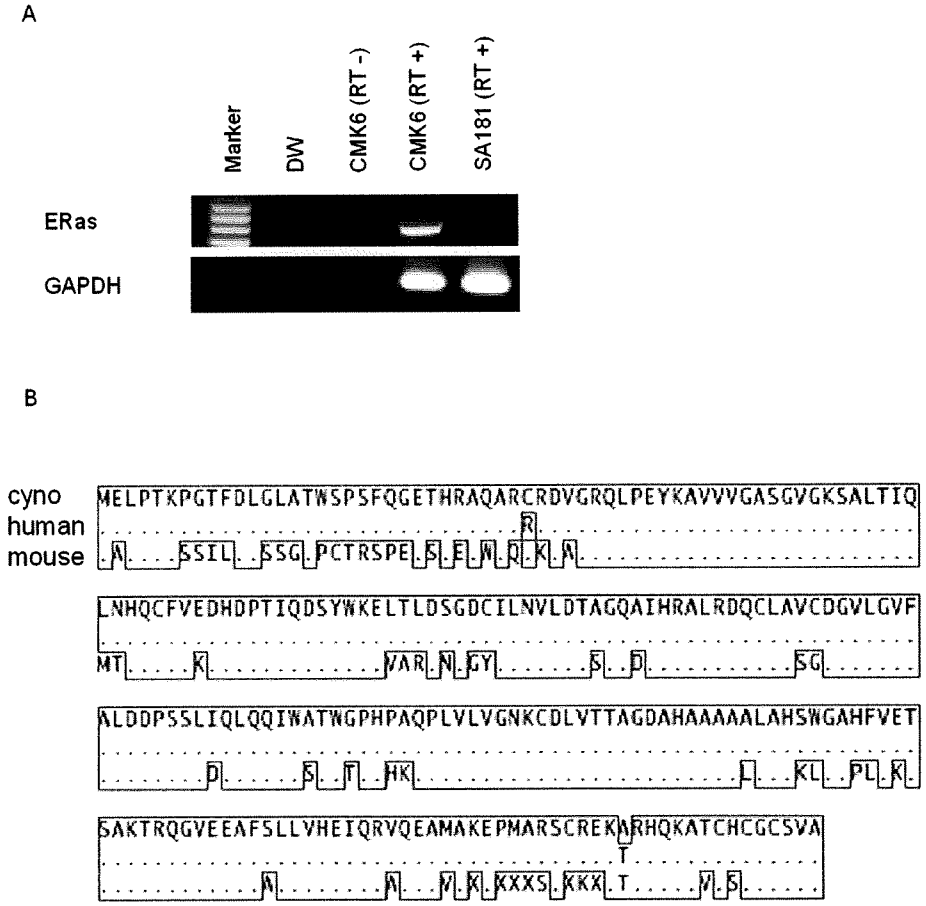

Figure 1. Cloning and sequencing of cynomolgus ERas. (A) The expression of the cynomolgus (cyno) ERas gene is detectable in cynomolgus ES cells (CMK6), but not in human ES cells (SA181), by reverse transcription (RT)-PCR. To exclude the possibility of genomic DNA contamination, PCR without the RT procedure (designated RT −) was also conducted. DW (distilled water) indicates no template in the reaction. RT-PCR of the GAPDH sequence is also shown as an internal control. (B) Amino acid sequences of cynomolgus, human (accession No. NM 181532), and mouse (accession No. NM 181548) ERas are shown. Amino acids identical to cynomolgus ERas are shown as dots and conserved amino acids are encircled with a solid line.

2D). We also tested mouse tissues, but ERas-positive cells were not detectable (Fig. 2C). Taken together, the ERas protein is indeed expressed in cynomolgus tissues, unlike in murine tissues.

The expression of the ERas gene becomes undetectable after the differentiation of mouse ES cells (22). We examined the expression of the ERas gene after the differentiation of cynomolgus ES cells. Cynomolgus ES cell-derived neurons and teratoma cells were examined for the expression of ERas as well as Oct-4, a pluripotent marker of ES cells. They were positive for ERas but negative for Oct-4 (Fig. 3A). Although cynomolgus ES cell-derived neurons were fragile and scarcely survived after dissociation from the culture dish, adherent teratoma cells could be cultured for more than six passages at a dilution of 1:4 to 1:8. Quantitative RT-PCR showed that the ERas gene expression levels were even higher in the cultured teratoma cells than in the undifferentiated cynomolgus ES cells (Fig. 3B). Then, we transplanted 1×10^7 cultured teratoma cells expressing the ERas gene (GFP-positive, passage 3) into the thigh muscle of NOG mice ($n = 3$), and examined the tumorigenicity of the cells. NOG mice were used as recipients, because they are more immunodeficient than other immunodeficient mice and transplanting to NOG mice is the most sensitive assay to detect tumorigenesis (7,14). However, no tumor developed after 2.5 months, although the transplanted cell progeny (GFP positive) were detected in every specimen (Fig. 3C). On the other hand, undifferentiated cynomolgus ES cells formed tera-

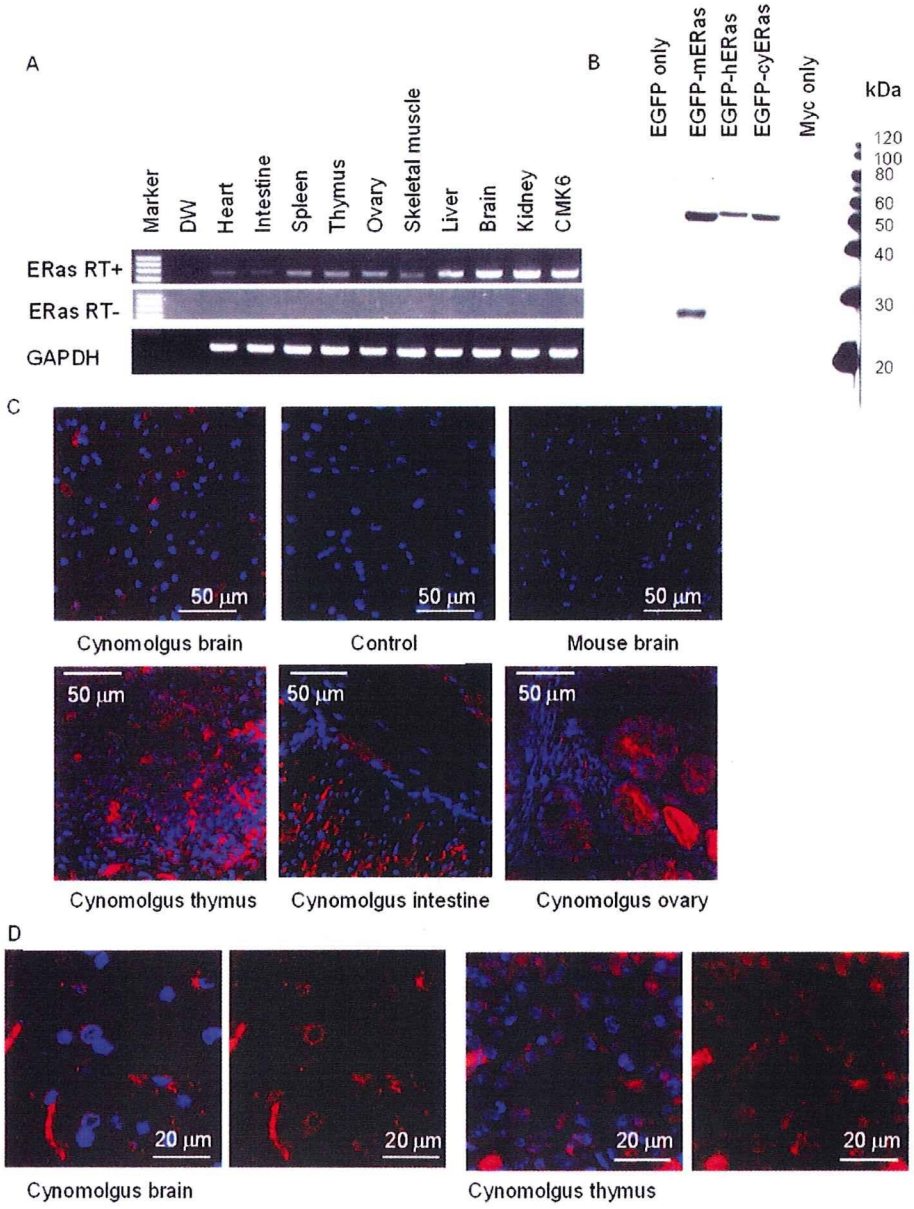

Figure 2. Cynomolgus tissues express ERas. (A) The expression of the cynomolgus ERas gene is detectable in various cynomolgus tissues by RT-PCR. To exclude the possibility of genomic DNA contamination, PCR without the RT procedure (designated RT –) was also conducted. DW indicates no template in the reaction. RT-PCR of the GAPDH sequence is also shown as an internal control. (B) Cynomolgus bone marrow stromal cells were transfected with the mouse ERas (mERas), human ERas (hERas), or cynomogus ERas (cyERas) gene fused with the EGFP gene, and immnunoblotted with the polyconal anti-ERas antibody. Although the antibody was generated against recombinant mERas (22), it reacts to hERas and cyERas as well as mERas. In addition, it does not react to cynomolgus other Ras family proteins (N-, H-, or K-Ras; 21 kDa). ERas (25 kDa) fused with EGFP (26 kDa) is detectable at 51 kDa. In mERas-transfected cells, ERas alone released from the fusion protein was also detected. (C) Using the anti-ERas antibody, ERas-positive cells (red) were detected in cynomolgus brain, thymus, intestine, and ovary. Control indicates the staining of cynomolgus brain without the primary ERas antibody. Although the primary antibody to ERas was originally developed for mouse ERas and should react more strongly to mouse than cynomolgus ERas, no positive signals were detected in mouse brain. (D) The ERas fluorescence with or without DAPI is shown at a higher magnification of both cynomolgus brain and thymus. ERas was detected on the cytoplasmic membrane.

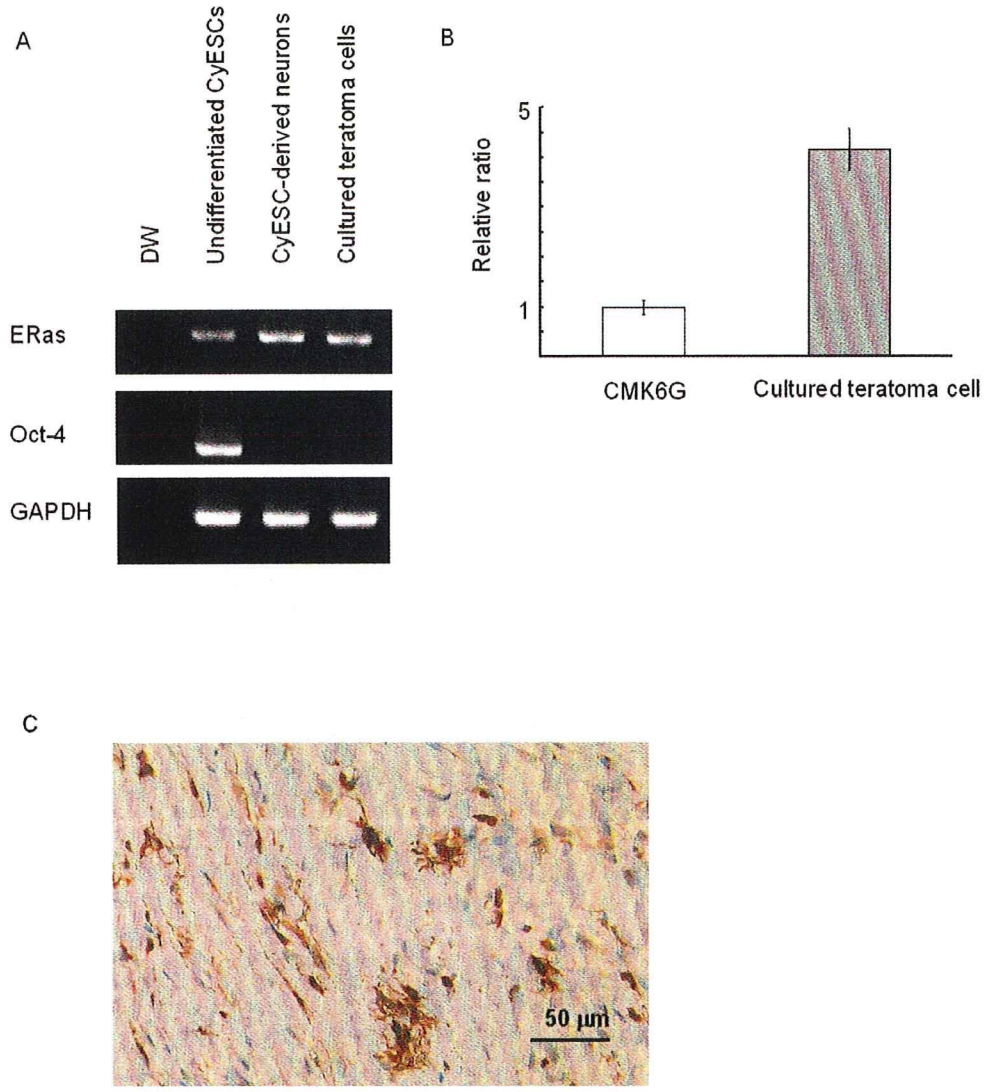

Figure 3. Cynomolgus ES cell-derived cells express ERas but do not form tumors in vivo. (A) The ERas gene was expressed in cynomolgus ES cell-derived neurons and teratoma cells as assessed by RT-PCR, whereas the Oct-4 gene was expressed in neither. DW indicates no template in the reaction. RT-PCR of the GAPDH sequence is also shown as an internal control. (B) The ERas gene expression level was nearly five times higher in the cultured teratoma cells than in the undifferentiated cynomolgus ES cells as assessed by quantitative RT-PCR. The gene expression level was adjusted using the internal control GAPDH. (C) The cultured teratoma cells were transplanted into the thigh muscles of NOG mice and examined for tumorigenicity in vivo after 2.5 months. Staining of the specimen with anti-GFP is shown. Although the transplanted cell progeny (GFP positive, brown) were detected, no tumor was observed.

tomas in all NOG mice. Taken together, cynomolgus ES cell-derived differentiated progeny and teratoma cells also express the ERas gene, but do not produce tumors in vivo.

ERas Overexpression in Cynomolgus Cells

To examine whether the cynomolgus ERas contributes to cell proliferation, we transfected cynomolgus stromal cells with a plamid expressing the cynomolgus or mouse ERas, EGFP, and puromycin resistance genes. Transfectants were obtained by treatment with puromycin and more than 90% of the cells expressed EGFP (Fig. 4A). These transfectants did not show significant morphological changes. Quantitative RT-PCR showed that the transfected cells expressed approximately 1000 times more ERas than undifferentiated cynomolgus ES

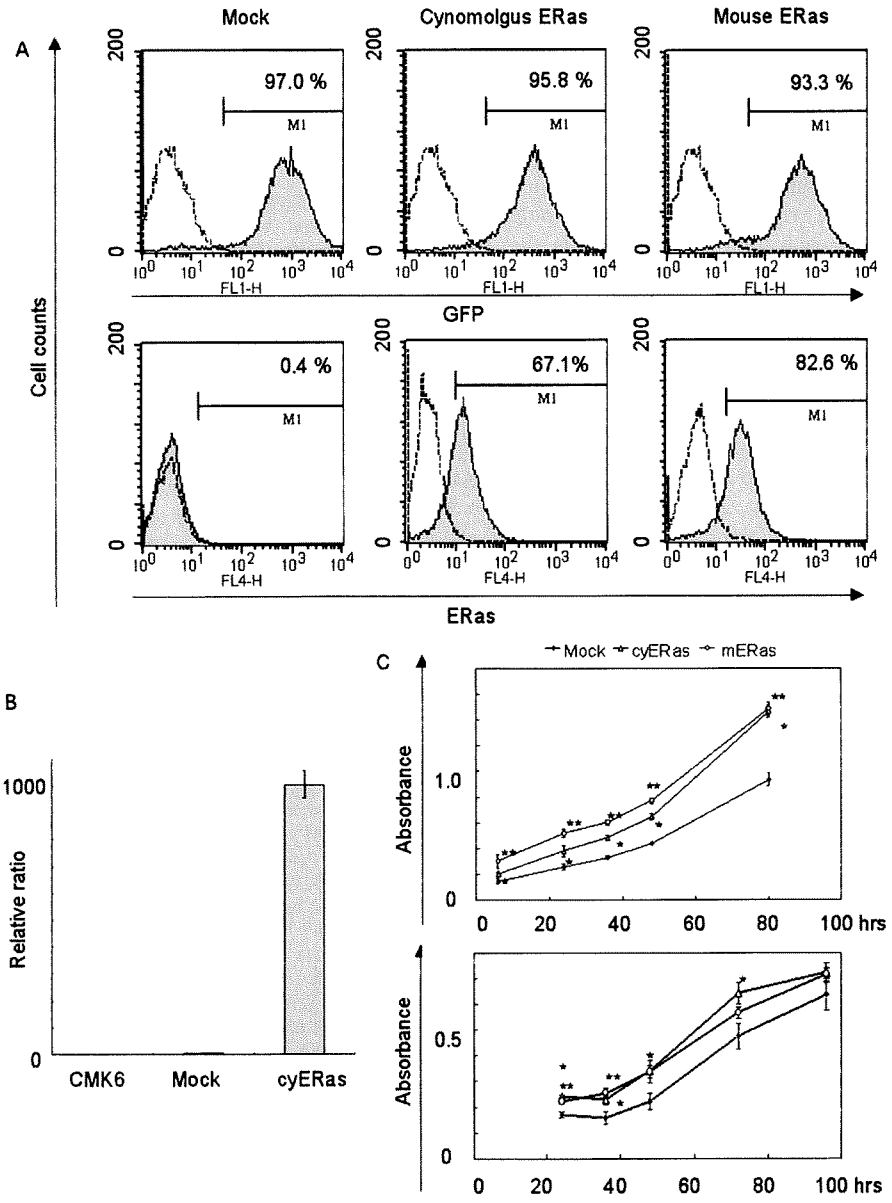

Figure 4. Overexpression of ERas does not promote cell proliferation but improves plating efficiency. (A) The plasmids expressing the cynomolgus or mouse ERas, EGFP, and puromycin resistance genes were transfected into cynomolgus stromal cells. After puromycin selection, more than 90% of cells expressed EGFP (upper). The ERas expression was also detected by flow cytometry (lower). (B) The level of cynomolgus ERas gene expression was 1000 times higher in the cynomolgus ERas-transfected cells (cyERas) than in naive cynomolgus ES cells (CMK6) or mock-transfected cells by quantitative RT-PCR. The gene expression levels were adjusted using the internal control GAPDH. (C) The mock-, cynomolgus ERas (cyERas)-, and mouse ERas (mERas)-transfected cells were plated at 5×10^3 per well and total cell numbers were measured after 6, 24, 36, 48, and 80 h of incubation (upper). The mock-, cyERas-, and mERas-transfected cells were plated at 2×10^3 per well and proliferating cell numbers were measured after 24, 36, 48, 72, and 96 h of incubation (lower). The cyERas- and mERas-transfected cells showed larger total cell or proliferating cell numbers after plating than the mock-transfected cells, but did not show any more rapid proliferation thereafter. Statistical differences with the *t*-test are indicated: $*p < 0.01$ for the cyERas- versus mock-transfected cells, $**p < 0.01$ for the mERas- versus mock-transfected cells.

cells (Fig. 4B). These cells expressing either cynomolgus or mouse ERas showed larger total cell numbers or proliferating cell numbers after plating than the mock-transfected cells, but did not show any more rapid proliferation thereafter (Fig. 4C). Thus, cynomolgus ERas improves plating efficiency but does not promote cell proliferation, even when it is expressed at high levels.

In this report, we showed that the cynomolgus ERas gene is expressed in cynomolgus ES cells and tissues. Its expression pattern is quite different from that of mouse ERas, which is not expressed in mouse ES cell-derived differentiated progeny or mouse tissues. Although cynomolgus ERas improved the plating efficiency when overexpressed, its expression did not promote cell proliferation or induce tumor formation in vivo (Figs. 3C, 4C). Thus, cynomolgus ERas might only suppress the apoptosis of cynomolgus cells (5). Because the formation of teratomas is one of the greatest obstacles to the clinical application of human ES cells (3,8,18), it is important to elucidate whether the ERas gene expressed in cynomolgus ES cells is related to teratoma development in vivo in order to tell whether nonhuman primate models are really suitable for preclinical research. From our study, it is at least suggested that cynomolgus ES cells are more similar to human than mouse ES cells in that ERas does not contribute to the formation of teratomas in vivo.

To date, the pluripotent marker Oct-4 has been used to predict the formation of teratomas (4) and the removal of Oct-4-positive cells from ES cell-derived progenitor preparations is reported to prevent teratomas from developing posttransplant (2). However, Oct-4-negative immature cells are also reported to contribute to the formation of teratomas (6). Therefore, although Oct-4 could be used to predict whether teratomas develop to some extent, it does not regulate the developmental process. For future clinical applications, the mechanism by which primate ES cells form teratomas should be studied in more detail.

ACKNOWLEDGMENTS: We thank Naomi Takino for technical assistance and Shuh-hei Fujishiro for helpful discussion. This study was supported by grants (JMS 21st Century COE Program, High-tech Research Center Program, and KAKENHI) from the Ministry of Education, Culture, Sports, Science and Technology of Japan as well as grants (KAKENHI) from the Ministry of Health, Labor and Welfare of Japan.

REFERENCES

1. Bhattacharya, B.; Miura, T.; Brandenberger, R.; Mejido, J.; Luo, Y.; Yang, A. X.; Joshi, B. H.; Ginis, I.; Thies, R. S.; Amit, M.; Lyons, I.; Condie, B. G.; Itskovitz-Eldor, J.; Rao, M. S.; Puri, R. K. Gene expression in human embryonic stem cell lines: unique molecular signature. Blood 103:2956–2964; 2004.
2. Bieberich, E.; Silva, J.; Wang, G.; Krishnamurthy, K.; Condie, B. G. Selective apoptosis of pluripotent mouse and human stem cells by novel ceramide analogues prevents teratoma formation and enriches for neural precursors in ES cell-derived neural transplants. J. Cell Biol. 167:723–734; 2004.
3. Bjorklund, L. M.; Sanchez-Pernaute, R.; Chung, S.; Andersson, T.; Chen, I. Y.; McNaught, K. S.; Brownell, A. L.; Jenkins, B. G.; Wahlestedt, C.; Kim, K. S.; Isacson, O. Embryonic stem cells develop into functional dopaminergic neurons after transplantation in a Parkinson rat model. Proc. Natl. Acad. Sci. USA 99:2344–2349; 2002.
4. Campbell, P. A.; Perez-Iratxeta, C.; Andrade-Navarro, M. A.; Rudnicki, M. A. Oct4 targets regulatory nodes to modulate stem cell function. PLoS ONE 2:e553; 2007.
5. Cox, A. D.; Der, C. J. The dark side of Ras: Regulation of apoptosis. Oncogene 22:8999–9006; 2003.
6. Dihne, M.; Bernreuther, C.; Hagel, C.; Wesche, K. O.; Schachner, M. Embryonic stem cell-derived neuronally committed precursor cells with reduced teratoma formation after transplantation into the lesioned adult mouse brain. Stem Cells 24:1458–1466; 2006.
7. Erdo, F.; Buhrle, C.; Blunk, J.; Hoehn, M.; Xia, Y.; Fleischmann, B.; Focking, M.; Kustermann, E.; Kolossov, E.; Hescheler, J.; Hossmann, K. A.; Trapp, T. Host-dependent tumorigenesis of embryonic stem cell transplantation in experimental stroke. J. Cereb. Blood Flow Metab. 23: 780–785; 2003.
8. Fujikawa, T.; Oh, S. H.; Pi, L.; Hatch, H. M.; Shupe, T.; Petersen, B. E. Teratoma formation leads to failure of treatment for type I diabetes using embryonic stem cell-derived insulin-producing cells. Am. J. Pathol. 166:1781–1791; 2005.
9. Hasegawa, K.; Fujioka, T.; Nakamura, Y.; Nakatsuji, N.; Suemori, H. A method for the selection of human embryonic stem cell sublines with high replating efficiency after single-cell dissociation. Stem Cells 24:2649–2660; 2006.
10. Heins, N.; Englund, M. C.; Sjoblom, C.; Dahl, U.; Tonning, A.; Bergh, C.; Lindahl, A.; Hanson, C.; Semb, H. Derivation, characterization, and differentiation of human embryonic stem cells. Stem Cells 22:367–376; 2004.
11. Hematti, P.; Obrtlikova, P.; Kaufman, D. S. Nonhuman primate embryonic stem cells as a preclinical model for hematopoietic and vascular repair. Exp. Hematol. 33:980–986; 2005.
12. Kameda, T.; Thomson, J. A. Human ERas gene has an upstream premature polyadenylation signal that results in a truncated, noncoding transcript. Stem Cells 23:1535–1540; 2005.
13. Kaufman, D. S.; Thomson, J. A. Human ES cells—haematopoiesis and transplantation strategies. J. Anat. 200: 243–248; 2002.
14. Kishi, Y.; Tanaka, Y.; Shibata, H.; Nakamura, S.; Takeuchi, K.; Masuda, S.; Ikeda, T.; Muramatsu, S.; Hanazono, Y. Variation in the incidence of teratomas after transplantation of nonhuman primate ES cells into immunodeficient mice. Cell Transplant. 17(9):1095–1102; 2008.
15. Nakayama, T.; Momoki-Soga, T.; Inoue, N. Astrocyte-derived factors instruct differentiation of embryonic stem cells into neurons. Neurosci. Res. 46:241–249; 2003.
16. Nakayama, T.; Momoki-Soga, T.; Yamaguchi, K.; Inoue, N. Efficient production of neural stem cells and neurons from embryonic stem cells. Neuroreport 15:487–491; 2004.
17. Rao, M. Conserved and divergent paths that regulate self-

renewal in mouse and human embryonic stem cells. Dev. Biol. 275:269–286; 2004.
18. Shibata, H.; Ageyama, N.; Tanaka, Y.; Kishi, Y.; Sasaki, K.; Nakamura, S.; Muramatsu, S.; Hayashi, S.; Kitano, Y.; Terao, K.; Hanazono, Y. Improved safety of hematopoietic transplantation with monkey embryonic stem cells in the allogeneic setting. Stem Cells 24:1450–1457; 2006.
19. Suemori, H.; Tada, T.; Torii, R.; Hosoi, Y.; Kobayashi, K.; Imahie, H.; Kondo, Y.; Iritani, A.; Nakatsuji, N. Establishment of embryonic stem cell lines from cynomolgus monkey blastocysts produced by IVF or ICSI. Dev. Dyn. 222:273–279; 2001.
20. Takada, T.; Suzuki, Y.; Kondo, Y.; Kadota, N.; Kobayashi, K.; Nito, S.; Kimura, H.; Torii, R. Monkey embryonic stem cell lines expressing green fluorescent protein. Cell Transplant. 11:631–635; 2002.
21. Takagi, Y.; Takahashi, J.; Saiki, H.; Morizane, A.; Hayashi, T.; Kishi, Y.; Fukuda, H.; Okamoto, Y.; Koyanagi, M.; Ideguchi, M.; Hayashi, H.; Imazato, T.; Kawasaki, H.; Suemori, H.; Omachi, S.; Iida, H.; Itoh, N.; Nakatsuji, N.; Sasai, Y.; Hashimoto, N. Dopaminergic neurons generated from monkey embryonic stem cells function in a Parkinson primate model. J. Clin. Invest. 115:102–109; 2005.
22. Takahashi, K.; Mitsui, K.; Yamanaka, S. Role of ERas in promoting tumour-like properties in mouse embryonic stem cells. Nature 423:541–545; 2003.
23. Tanaka, Y.; Nakamura, S.; Shibata, H.; Kishi, Y.; Ikeda, T.; Masuda, S.; Sasaki, K.; Abe, T.; Hayashi, S.; Kitano, Y.; Nagao, Y.; Hanazono, Y. Sustained macroscopic engraftment of cynomolgus embryonic stem cells in xenogeneic large animals after in utero transplantation. Stem Cells Dev. 17:367–382; 2008.
24. Thomson, J. A.; Kalishman, J.; Golos, T. G.; Durning, M.; Harris, C. P.; Becker, R. A.; Hearn, J. P. Isolation of a primate embryonic stem cell line. Proc. Natl. Acad. Sci. USA 92:7844–7848; 1995.
25. Wolf, D. P. Nonhuman primate embryonic stem cells: An underutilized resource. Regen. Med. 3:129–131; 2008.

OPEN ACCESS Freely available online

PLoS one

Self-Contained Induction of Neurons from Human Embryonic Stem Cells

Tsuyoshi Okuno[1,2], Takashi Nakayama[3], Nae Konishi[1], Hideo Michibata[1], Koji Wakimoto[1], Yutaka Suzuki[1], Shinji Nito[1], Toshio Inaba[2], Imaharu Nakano[4], Shin-ichi Muramatsu[4], Makoto Takano[5], Yasushi Kondo[1]*, Nobuo Inoue[6]

1 Advanced Medical Research Laboratory, Mitsubishi Tanabe Pharma Corporation, Osaka, Japan, **2** Department of Advanced Pathobiology, Graduate School of Life and Environmental Sciences, Osaka Prefecture University, Osaka, Japan, **3** Department of Biochemistry, Yokohama City University School of Medicine, Yokohama, Japan, **4** Division of Neurology, Department of Medicine, Jichi Medical University, Tochigi, Japan, **5** Department of Physiology, Jichi Medical University, Tochigi, Japan, **6** Laboratory of Regenerative Neurosciences, Graduate School of Human Health Sciences, Tokyo Metropolitan University, Tokyo, Japan

Abstract

Background: Neurons and glial cells can be efficiently induced from mouse embryonic stem (ES) cells in a conditioned medium collected from rat primary-cultured astrocytes (P-ACM). However, the use of rodent primary cells for clinical applications may be hampered by limited supply and risk of contamination with xeno-proteins.

Methodology/Principal Findings: We have developed an alternative method for unimpeded production of human neurons under xeno-free conditions. Initially, neural stem cells in sphere-like clusters were induced from human ES (hES) cells after being cultured in P-ACM under free-floating conditions. The resultant neural stem cells could circumferentially proliferate under subsequent adhesive culture, and selectively differentiate into neurons or astrocytes by changing the medium to P-ACM or G5, respectively. These hES cell-derived neurons and astrocytes could procure functions similar to those of primary cells. Interestingly, a conditioned medium obtained from the hES cell-derived astrocytes (ES-ACM) could successfully be used to substitute P-ACM for induction of neurons. Neurons made by this method could survive in mice brain after xeno-transplantation.

Conclusion/Significance: By inducing astrocytes from hES cells in a chemically defined medium, we could produce human neurons without the use of P-ACM. This self-serving method provides an unlimited source of human neural cells and may facilitate clinical applications of hES cells for neurological diseases.

Citation: Okuno T, Nakayama T, Konishi N, Michibata H, Wakimoto K, et al. (2009) Self-Contained Induction of Neurons from Human Embryonic Stem Cells. PLoS ONE 4(7): e6318. doi:10.1371/journal.pone.0006318

Editor: Tailoi Chan-Ling, University of Sydney, Australia

Received June 3, 2008; **Accepted** June 24, 2009; **Published** July 21, 2009

Funding: Part of this work was supported by grants from the Ministry of Education, Science, Sports and Culture, the Japanese Government; and from the Japan Ministry of Health, Labor and Welfare.

Competing Interests: The authors have declared that no competing interests exist.

* E-mail: kondo.yasushi@mc.mt-pharma.co.jp

Introduction

Embryonic stem (ES) cells, derived from the inner cell mass of blastocysts, are pluripotent cells that can differentiate into a variety of cell types including neural cells [1,2]. Among the various basic and clinical applications for ES cells, cell transplantation therapy for central nervous diseases is of particular interest because differentiated neurons do not proliferate, and a relatively large number of donor cells are necessary to replace diseased neurons. Several methods have been developed to prepare neural cells from ES cells. Neurons can be obtained indirectly from ES cells via ectodermal cells in embryoid bodies, which are formed from dissociated ES cells, either by induction with retinoic acid or selection [3,4]. Alternatively, neural stem cells and neurons can be directly differentiated from ES cells without forming embryoid bodies by culturing ES cells on mouse-cultured stroma cells (PA-6) [5], or under chemically defined low-density culture conditions [6]. All of these procedures, however, are time consuming and require highly complicated processes to generate many neurons. In addition, their practicality is limited by the possible teratogenicity caused by culture factors, such as retinoic acid, of differentiated cells. We have previously reported an efficient method to prepare transplantable neural cells from mouse ES cells using a conditioned medium collected from rat primary-cultured astrocytes (P-ACM) [7–9]. In this study, we applied this method to human ES (hES) cells for induction of neurons and astrocytes. Once the astrocytes were derived from hES cells, they could be substituted for primary astrocytes that induce neurons, thus achieving xeno-free production of neurons.

Results

Neural cell differentiation from hES

Four hES cell-lines stably expressing humanized renilla green fluorescent protein (hrGFP) were obtained. These hES cell-lines were kept in undifferentiated state with positive stem cell markers, such as alkaline phosphatase, Oct-4, and SSEA-4. When cultured

in P-ACM containing fibroblast growth factor-2 (FGF-2) under free-floating conditions, colonies of undifferentiated hES cells gave rise to floating spheres composed of neural stem cells and undifferentiated cells, which gradually increased in size during the culture. After 12 days of culture, the spheres were plated onto a poly-L-Lysine/Laminin coated dish and cultivated in neural stem cell medium (NSCM) containing high concentrations of FGF-2 and epidermal growth factor (EGF). Within 24 h, the spheres attached onto the substrate and formed circular clusters of cells. Many of these cells subsequently migrated to the surrounding areas and covered the growth surface of the dish in circular monolayers. After replacing NSCM by P-ACM and culture for 14 days, the spheres differentiated into neurons (Figures 1A, B) and few astrocytes (Figures 1C). These were identified by the neuronal marker tubulin β III isoform (Tuj1) and the astrocytic marker glial fibrillary acidic protein (GFAP).

Selective differentiation of hES cells into neurons and astrocytes

By culture of the spheres in NSCM, neural stem cells were able to migrate from the attached spheres to the surrounding area and subsequently form a circular cluster. NSCM containing FGF-2 and EGF promotes neural stem cells proliferation, while repressing their differentiation into any type of neural cells. After removing the core of the attached spheres mechanically, the remaining neural stem cells could proliferate in NSCM and selectively differentiate into neurons and astrocytes by subculture in an appropriate medium. To differentiate into neurons, neural stem cells were subcultured using 0.05% Trypsin/EDTA in P-ACM for 14 days (Figures 2A, B). After these 14 days of subculture, a large number of cells expressed Tuj1 ($84.0 \pm 5.1\%$, $n = 3$). On the other hand, to differentiate into astrocytes, neural stem cells were subcultured in G5 medium for 14 days (Figure 2C). After this subculture, a large number of cells expressed

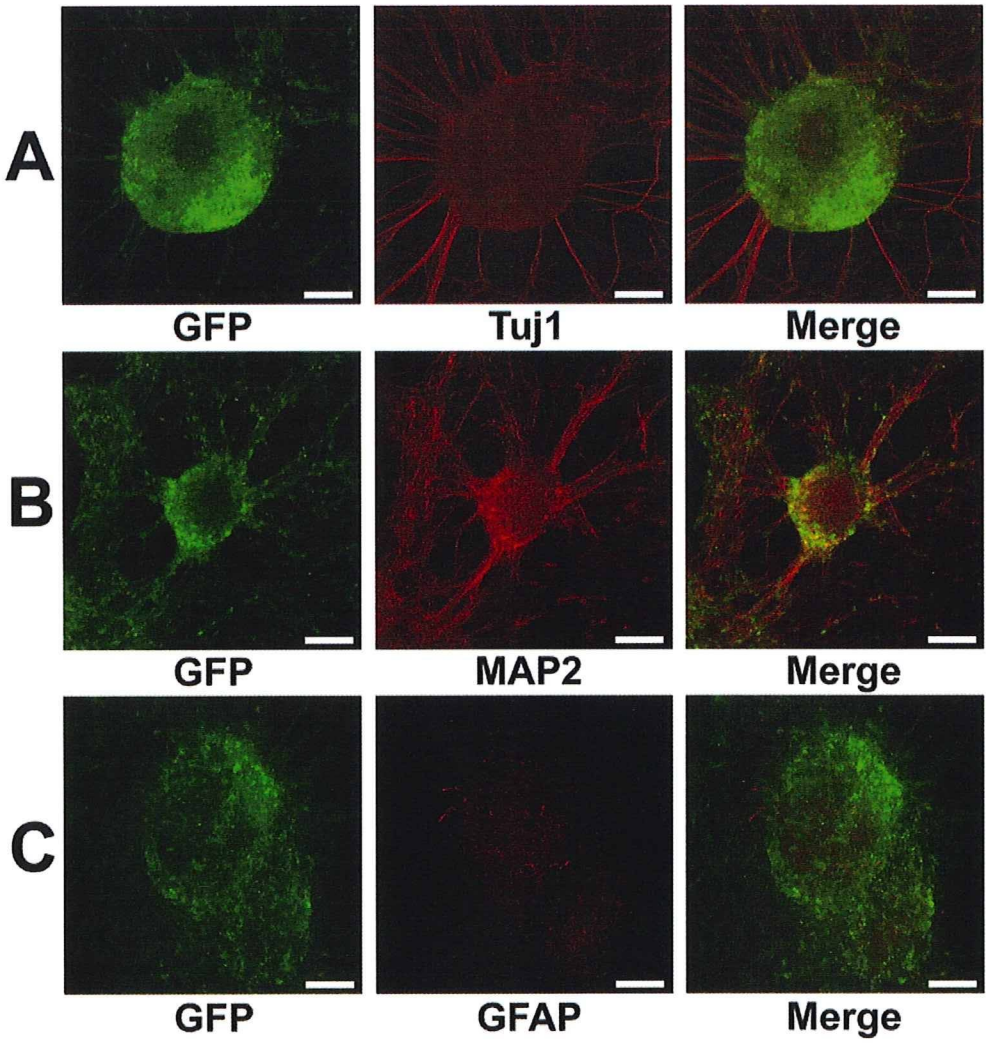

Figure 1. Differentiation of hES cells into neurons in P-ACM. Floating spheres composed of neural stem cells and undifferentiated cells grown for 12 days were plated on an adhesive substrate and cultured for 14 days in P-ACM. Expression of hrGFP (green), Tuj1 (A, red), MAP2 (B, red), and GFAP (C, red) staining of the many neural and few glial cells derived from hES cells. Bar = 100 μm.
doi:10.1371/journal.pone.0006318.g001

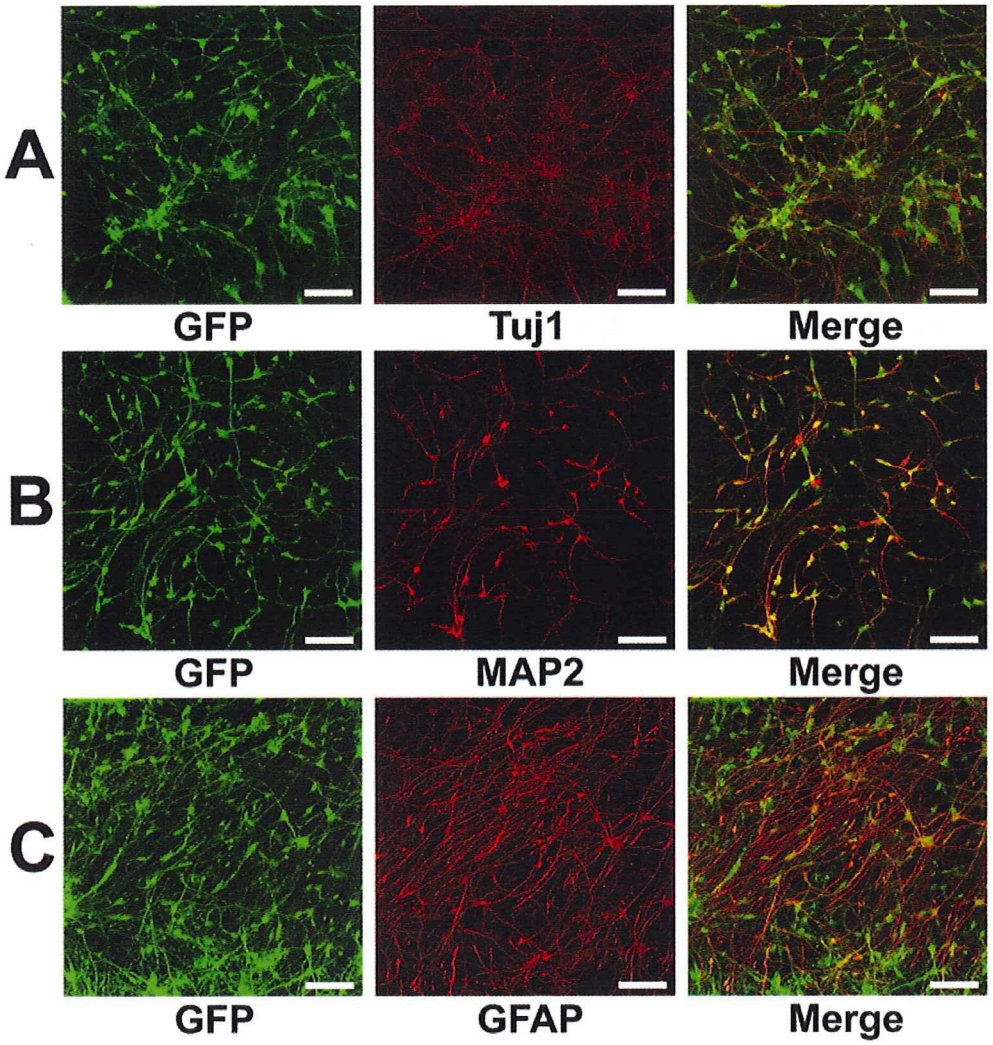

Figure 2. Selective induction of hES cells into neurons and astrocytes. (A, B): Neural stem cells that had migrated from floating spheres in NSCM were subcultured onto a PLL coated plate and cultured for 14 days in P-ACM. Immunostaining with antibody to Tuj1 and MAP2 showed that the subcultured neural stem cells had differentiated into neurons. Expression of hrGFP (green), (A) Tuj1 (red), and (B) MAP2 (red) staining profiles. (C): Neural stem cells were cultured for 14 days after removal of the core of spheres with a glass pipette and change of medium to G5 medium. The proliferated cells were subcultured onto PLL/LAM coated plate and cultured for 14 days in G5 medium. Immunostaining with antibody to GFAP showed that the subcultured cells had differentiated into astrocytes. Expression of hrGFP (green) and GFAP (red) staining profiles. Bar = 100 μm.
doi:10.1371/journal.pone.0006318.g002

GFAP (75.0±1.2%, $n = 3$). The removed core of the attached spheres could, like the first spheres, be used repeatedly (about twenty times) as seed for neural stem cells.

Xeno-free induction of astrocytes using a chemically defined medium

For collection of xeno-free astrocytes derived from hES cells, we used a chemically defined N2 medium for neural induction. When cultured in N2 medium containing FGF-2 and EGF under free-floating conditions, colonies of undifferentiated hES cells gave rise to floating spheres. As N2 was less efficient than P-ACM for obtaining astrocytes, we prepared hES cells in large scale ($>10^8$ cells). After differentiation, millions of astrocytes were gained under xeno-free condition (Figure 3A).

Neuronal induction of hES cell-derived astrocytes

Next, we investigated whether the astrocytes derived from hES cells can be substituted for primary astrocytes to differentiate hES cells into neural cells. A conditioned medium of hES cell-derived astrocytes was collected after two days culture and used as ES-ACM by adding an equal amount of N2 medium. As in the case of P-ACM, hES cells cultured in ES-ACM differentiated into neural cells via formation of spheres. After switching the cells from NSCM to ES-ACM, many cells had neuronal-like appearance with long neurites. By 6 weeks of culture in ES-ACM, most cells had neural morphology and expressed microtubule-associated protein 2 (MAP2) (Figure 3B). During our procedure for differentiating hES cells using ES-ACM, expression of several markers was analyzed by RT-PCR (Figure 4A). By 8 weeks culture

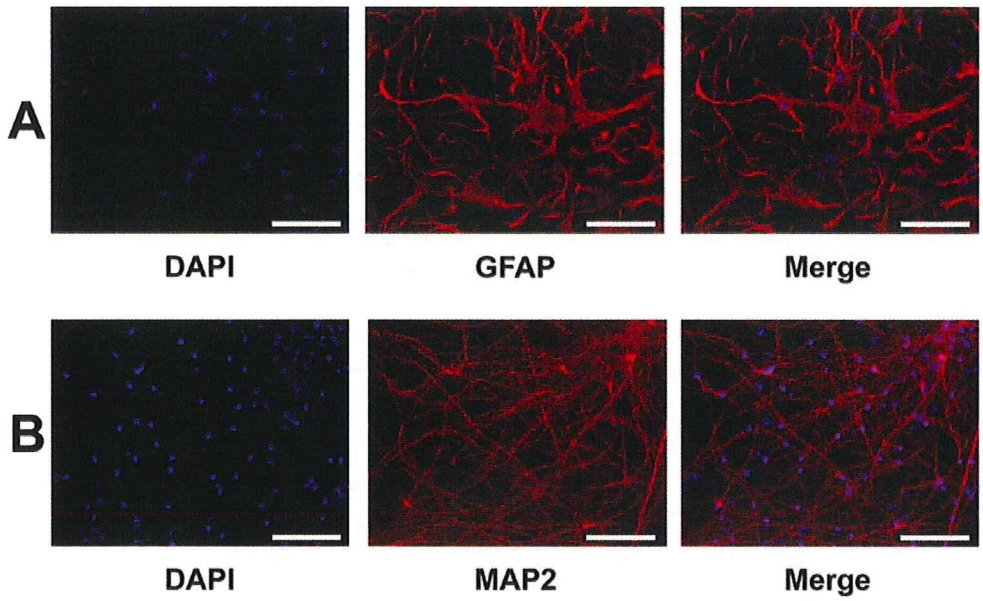

Figure 3. Differentiation of hES cells into astrocytes in a chemically defined medium. (A): Neural stem cells induced by N2 medium were cultured for 14 days after removal of the core of spheres with a glass pipette and change of medium to G5 medium. The proliferated cells were subcultured onto a PLL/LAM coated plate and cultured for 14 days in G5 medium. Immunostaining with antibody to GFAP showed that most of the subcultured cells had differentiated into astrocytes. DAPI (blue) and GFAP (green) staining profiles. Neural stem cells induced by xeno-free ES-ACM were subcultured onto PLL coated plate and cultured for 6 weeks in ES-ACM. (B): Immunostaining with antibody to MAP2 showed that the subcultured NSCs had differentiated into mature neurons. DAPI (blue) and MAP2 (red) staining profiles. Bar = 100 μm.
doi:10.1371/journal.pone.0006318.g003

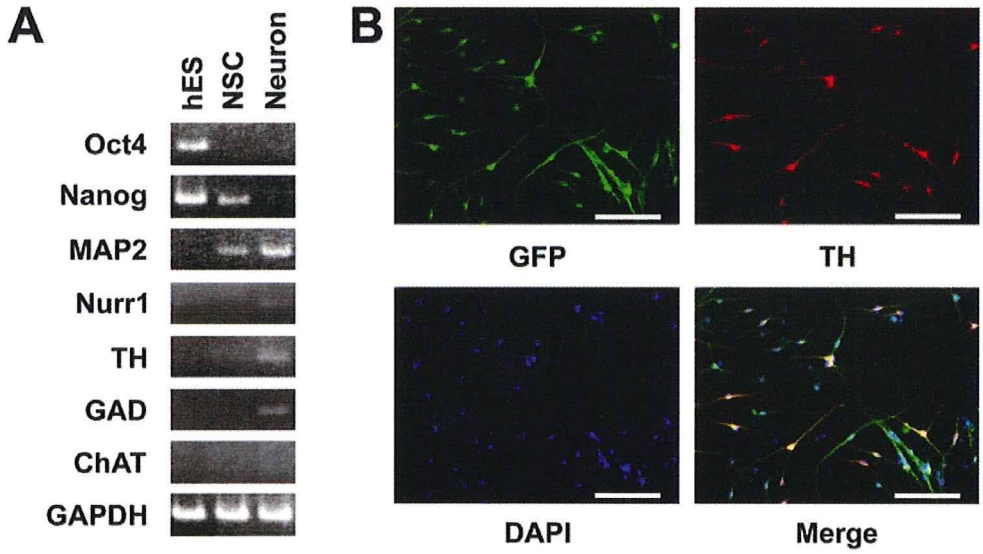

Figure 4. RT-PCR analysis and differentiation of hES cells into dopaminergic neurons in xeno-free ES-ACM. (A): RT-PCR analysis of hES cells, neural stem cells and mature neurons. RNA was isolated from clones of undifferentiated hES cells, from neural stem cells, and from mature neurons which had been cultured for 8 weeks in ES-ACM and analyzed for expression of marker genes. The expression levels of each gene were normalized to GAPDH gene expression level. hES, undifferentiated hES cells; NSC, neural stem cells; Neuron; mature neurons. (B): Differentiation of hES cells into dopaminergic neural cells in xeno-free ES-ACM. Neural stem cells induced by ES-ACM were subcultured onto PLL coated plate and cultured for 8 weeks in ES-ACM. Immunostaining with antibody TH and expression of hrGFP showed that the subcultured neural stem cells had differentiated into dopaminergic neurons. Expression of hrGFP (green), DAPI (blue) and TH (red) staining profiles. Bar = 100 μm.
doi:10.1371/journal.pone.0006318.g004